Bruno Exposto, Vítor Monteiro, J. G. Pinto, Delfim Pedrosa, Andrés A. Nogueiras Meléndez, João L. Afonso

"Three Phase Current Source Shunt Active Power Filter with Solar Photovoltaic Grid Interface"

IEEE ICIT Industrial Technology Conference, pp.1211-1215, Seville, Spain, March 2015.

http://ieeexplore.ieee.org/stamp/stamp.jsp?tp=&arnumber=7125262

ISBN: 978-1-4799-7799-4

DOI 10.1109/ICIT.2015.7125262

Bruno Exposto, Vítor Monteiro, J. G. Pinto, Delfim Pedrosa, Andrés A. Nogueiras Meléndez, João L. Afonso "Three Phase Current Source Shunt Active Power Filter with Solar Photovoltaic Grid Interface" IEEE ICIT Industrial Technology Conference, pp.1211-1215, Seville, Spain, March 2015. ISBN: 978-1-4799-7799-4 DOI 10.1109/ICIT.2015.7125262

Three-Phase Current-Source Shunt Active Power Filter with Solar Photovoltaic Grid Interface

Bruno Exposto[1], Vítor Monteiro[1], J. G. Pinto[1], Delfim Pedrosa[1], Andrés A. Nogueiras Meléndez[2], João L. Afonso[1]
[1]ALGORITMI Research Centre – University of Minho, Guimarães – Portugal
[2]Departamento de Tecnología Electrónica – University of Vigo, Vigo – Spain
[1]{bruno.exposto | vitor.monteiro | gabriel.pinto | delfim.pedrosa | joao.l.afonso}@algoritmi.uminho.pt [2]aaugusto@uvigo.es

***Abstract* – This paper presents the proposal of a three-phase current-source shunt active power filter (CS-SAPF) with photovoltaic grid interface. The proposed system combines the compensation of reactive power and harmonics with the injection of energy from a solar photovoltaic array into the electrical power grid. The proposed equipment presents the advantage of giving good use to the current-source inverter, even when the solar photovoltaic array is not producing energy. The paper describes the control system of the CS-SAPF, the energy injection control strategy, and the current harmonics and power factor compensation strategy. Simulation results to assess the performance of the proposed system are also presented.**

Keywords—Power Quality; Harmonics Compensation; Power Factor Correction; Solar Photovoltaics; Current-Source Inverter.

I. INTRODUCTION

Climate change and the problems associated with the use of fossil fuels are forcing the shift to new energy sources. Renewable energy sources are a good alternative to conventional energy sources, because they present a lower environmental impact, and take advantage of natural resources. Renewable energy expansion is a trend in Europe and generally in all the world. The European Union goals in terms of the use of renewable energy sources are 20% renewable energy share in energy consumption by 2020 [1]. China, United States, and other countries are pursuing similar goals, with China aiming to a share of 15% to the total primary energy in 2020 [2] and United States with incentives both in state scope or federal scope to renewable energy use [3][4].

Solar photovoltaic is one of the renewable energy sources that has been more increasingly explored. Over the years solar photovoltaic technology has been developed and the prices either of the solar photovoltaic panels, as well as the price of the power converters, have been consistently lowering [2][5]. Today's solar photovoltaic systems integrate a solar array and power electronics systems that allow perform the power conversion from the solar photovoltaic arrays to the electrical grid. In an isolated system, the system is connected directly to the loads. Generically this system integrates a dc-dc power converter and a dc-ac power converter. The dc-ac converter is connected to the electrical grid using first or second order passive filters. Solar photovoltaic systems can be therefore classified in terms of power and in terms of the type of power converters that constitute it [3].

The main adopted inverter topology is the voltage-source inverter. Nevertheless there has been made some research with current-source inverters applied to solar photovoltaic systems [6][7]. Current-source inverters have been used in other power electronics applications such as active filters, motor drives and renewable energy applications [8][9]. The advantages of this type of inverter are the good quality output currents and the fact of being robust [10]. The disadvantages are the bulky dc-link inductance, and the increased dc-link energy losses.

In this paper is proposed the use of a current-source shunt active power filter (CS-SAPF) to perform the interface between the electrical grid and a solar photovoltaic array. The control of the CS-SAPF, alongside with the energy injection capability, also integrates low power factor compensation, and current harmonics compensation.

II. CS-SAPF WITH SOLAR PHOTOVOLTAIC INTERFACE TOPOLOGY

The topology of the proposed current-source inverter is constituted by a three-phase current-source inverter and a step-up converter connected to the dc-link (Fig. 1). The power switches in the inverter are RB-IGBTs. This is necessary

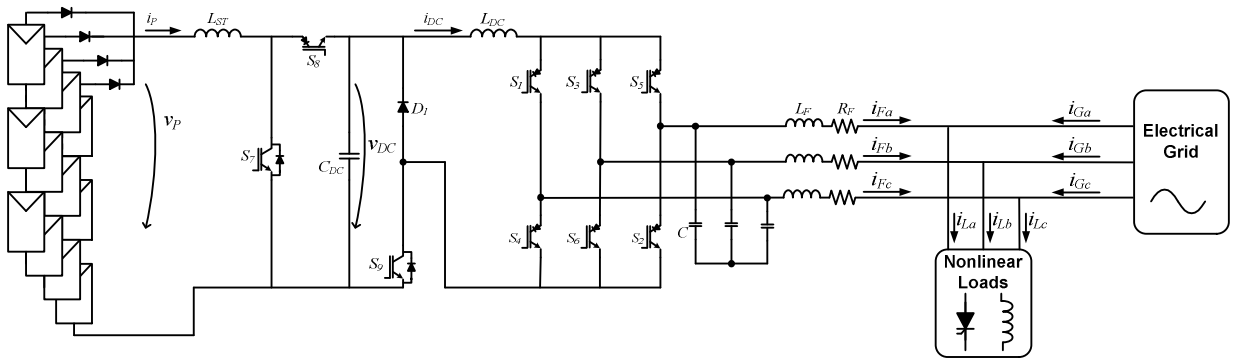

Fig. 1. Topology of the proposed three-phase current-source shunt active power filter (CS-SAPF) with solar photovoltaic grid interface.

because in a current-source inverter, the power switches must withstand direct and reverse voltages. In the dc-dc converter, *S7* is a conventional IGBT and *S8* is a RB-IGBT.

The three-phase current-source inverter is responsible by inject energy into the electrical grid and, at the same time, inject reactive energy into the grid, and compensate current harmonics generated by a nonlinear load, placed in parallel with the inverter. The compensation is performed measuring the nonlinear load currents $i_{L\{a,b,c\}}$.

The operation of the dc-link step-up converter is divided in two steps represented in Fig. 2. In the first step, *S7* and S9 are on. In this state, the current of the panels (i_P) flows through L_{ST} and S9 injecting energy in the dc-link inductance. At the same time, the current of the dc-link (i_{DC}) flows through the capacitor CDC. In the second step, *S7* and *S9* are off, and the current of the panels (i_P) flows through the capacitor C_{DC}, charging it again. In this way is possible to have more current in the dc-link or less, than the maximum power point (MPP) current of the panels. This enables the reactive energy injection, and load current harmonics compensation with large amplitudes, while injecting energy into the electrical grid.

The interface between the dc-dc converter and the dc-link of the CS-SAPF is done using *S9* and *D1*. This interface is a voltage-to-current converter similar to what is used in [11]. This circuit is a voltage-to-current converter, which is responsible for transferring the energy stored in capacitor to the dc-link inductor of the CS-SAPF. This circuit allows the flow of the dc-link current either by the diode *D1*, when the capacitor C_{DC} is being charged with the energy that comes from the solar photovoltaic array, or discharge it by making flow the current through *S9*.

A. Grid Energy Injection and Compensation Strategy

In order to inject energy into the electrical grid, is necessary convert the dc current produced by the panels into ac current,

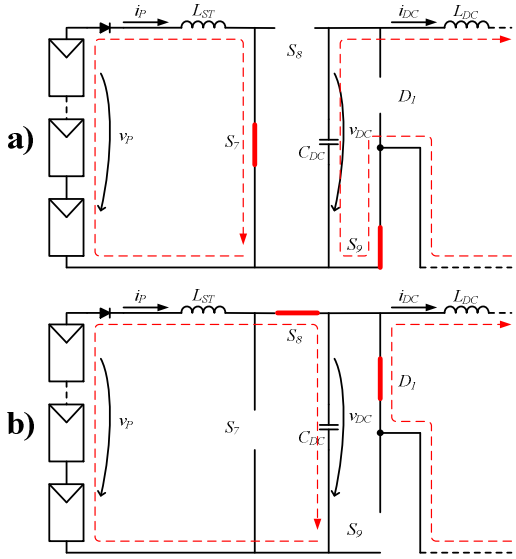

Fig. 2. Dc-dc converter operation: (a) Discharging of the output capacitor; (b) Charging of the output capacitor.

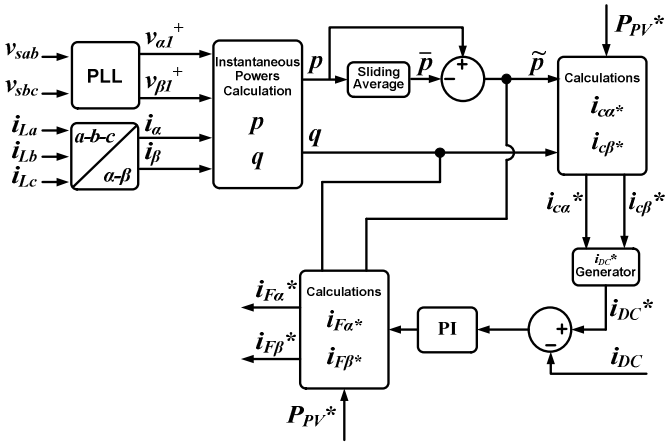

Fig. 3. Block diagram of the CS-SAPF controller.

in this case three-phase ac current. Also, is necessary ensure that the maximum power is extracted from the panels in every moment. To deal with all this features at the same time that is injected reactive energy and are compensated the load harmonics, was implemented the control algorithm depicted in Fig. 3. To detect the harmonics and generate the references was implemented a control based in the *p*-*q* Theory. This power theory was extensively used in active filters [12][13].

To determine the reference currents $i_{F\alpha}$ and $i_{F\beta}$ is necessary in the first place calculate *p* and *q*:

$$\begin{bmatrix} p \\ q \end{bmatrix} = \begin{bmatrix} v_\alpha^+ & v_\beta^+ \\ v_\beta^+ & -v_\alpha^+ \end{bmatrix} \begin{bmatrix} i_\alpha \\ i_\beta \end{bmatrix}. \tag{1}$$

After the compensation, only the average value of the instantaneous real power ($\bar{p}$) is desirable, and the other power components must be compensated. So to ensure this, is determined the average of *p*:

$$\bar{p} = \frac{1}{T}\int p(t)\ dt \ . \tag{2}$$

The mean value of p is then calculated subtracting the average value to *p* as:

$$\tilde{p} = p - \bar{p}. \tag{3}$$

The reference dc-link current, i_{DC}*, is calculated using $\tilde{p}$, *q* and P_{PV}. It must be referred that P_{PV} is the instantaneous power in the input of the dc-dc converter. After calculating $i_{c\alpha}$ and $i_{c\beta}$, the dc-link reference current is calculated using:

$$i_{DC}^* = K\sqrt{i_{c\alpha}^{\ 2} + i_{c\beta}^{\ 2}}\ . \tag{4}$$

The control of the dc-link current is performed by a proportional-integral (PI) controller. In this way, the CS-SAPF is constantly injecting the energy produced by the solar photovoltaic panels into the electrical grid. It must be referred that the output currents of the inverter are feedbacked to the control. Nevertheless, because the inverter is current-source

type, the control can be open-loop. This is similar to what is done in .

B. Maximum Power Point Tracker Algorithm

The adopted maximum power point tracker (MPPT) algorithm was Incremental Conductance. This method, although is more complex than other methods, has a good performance [14]. Furthermore, this is a true MPPT and when the maximum power point (MPP) is reached, the algorithm stays in that operating point, until is detected some change. To implement this algorithm is necessary measure the photovoltaic array output voltage (v_P) and output current (i_P). In Fig. 4 is possible to see the flowchart of the implemented MPPT algorithm. The MPPT algorithm controls directly the duty-cycle imposed to the dc-dc converter.

C. Resonance Damping Strategy

Considering that the passive filters of a current-source inverter are usually of type CL, which are second-order passive filters, this leads to a second-order system, with a defined resonance frequency. Therefore in the control of the inverter must be integrated mechanisms to damp the resonance caused by the passive filters. One strategy similar to that is done in [15], consists in calculate a damping current based in the predicted current that flows in the capacitor, and subtract it to the reference current. To implement this strategy the current that flows in the capacitor can be expressed as:

$$i_{CP\{\alpha,\beta\}} = C\frac{dv_{G\{\alpha,\beta\}}}{dt} + CL_F\frac{d^2 i_{F\{\alpha,\beta\}}}{dt^2} + CR_F\frac{di_{F\{\alpha,\beta\}}}{dt} \quad (5)$$

Making: $i_{F\{\alpha,\beta\}} = i^*_{F\{\alpha,\beta\}}$, its possible predict the capacitor current (i_{CP}) as in (6).

$$i_{CP\{\alpha,\beta\}} = C\frac{dv_{G\{\alpha,\beta\}}}{dt} + CL_F\frac{d^2 i^*_{F\{\alpha,\beta\}}}{dt^2} + CR_F\frac{di^*_{F\{\alpha,\beta\}}}{dt} \quad (6)$$

In Fig. 1 is possible to see that the capacitor current depends of the output current and the grid voltage. The part originated by the grid voltage can be compensated injecting a constant reactive power value ($\bar{q}$) in the reference currents generation. So to compensate only the transitory caused by the variation of the reference current, can reduced to:

$$i_{CP\{\alpha,\beta\}} = CL_F\frac{d^2 i^*_{F\{\alpha,\beta\}}}{dt^2} + CR_F\frac{di^*_{F\{\alpha,\beta\}}}{dt} \quad (7)$$

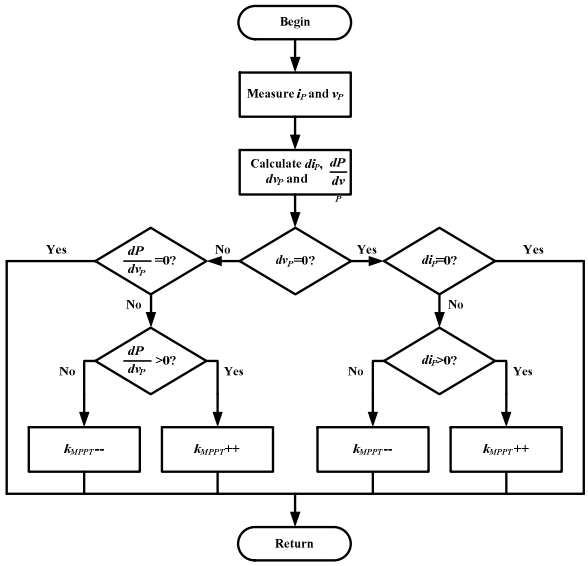

Fig. 4. Implemented MPPT algorithm (Incremental Conductance).

This method has the advantage of not require any extra current or voltage sensors. The disadvantage is that if the parameters of the model vary, the method will lose performance.

To complement the aforementioned damping method was also implemented a virtual harmonic damper. To do this, are calculated the distorted components voltage using the grid voltages subtracted to the phase-locked loop (PLL) and the output reference current as:

$$i_{DV\{\alpha,\beta\}} = -\frac{1}{R_h}(v_{G\{\alpha,\beta\}} - v^+_{\{\alpha,\beta\}}) \quad (8)$$

Considering that the grid voltages usually are distorted, if we subtract the (PLL) generated voltages to the measured grid voltages, the result signal will be resulting by the grid voltage distortion caused by the loads and the dynamics of the passive filters. The combination of the two aforementioned strategies can be seen in Fig. 5. It must be referred that (7) and (8) are discretized so that can be implemented in the digital controller.

Finally, the reference current that includes the damping current, the solar photovoltaic injecting current and the load compensating current, is sent to the space-vector modulation block. This block determine the sector where is located the current reference vector and the switching times. Then compares the times with a saw-tooth wave and places the inverter in the states that are necessary to synthetize the reference current. The switching frequency of the inverter is 32 kHz.

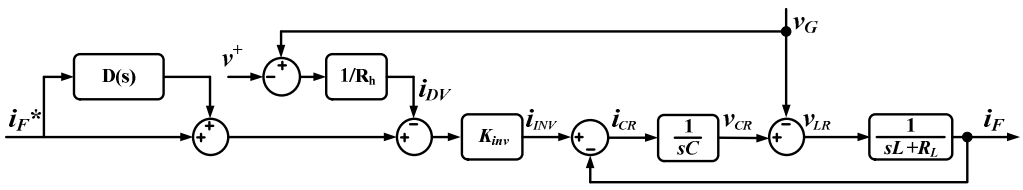

Fig. 5. Damping loop applied to the current-source shunt active power filter (CS-SAPF).

III. Simulation Results

In order to determine the performance of the proposed CS-SAPF with solar photovoltaic interface, was developed a simulation model similar to what is depicted in Fig. 1. The model parameter values are shown in Table I.

The load is constituted by a three-phase full-bridge rectifier with a RL(R=26 Ω, *L*=146 mH) placed in the dc-link and a three-phase balanced RL (*R*=23 Ω, *L*=95 mH) load. These two loads were chosen because the resulting currents will be distorted and the power factor will be low.

In Fig. 6 can be seen the simulation results of the CS-SAPF when compensates the load at the same time it injects energy in to the grid. As can be seen, in Fig. 6 (a), the source currents are sinusoidal and in phase with the voltages. The CS-SAPF injects currents (Fig. 6 (b)) that compensate the load currents Fig. 6 (c). The figure also shows that the source current amplitudes are inferior to the load currents. This demonstrates that the reactive power is being compensated. Also, this attests that the solar photovoltaic generated energy is being injected into the electrical grid lowering the rms value of the source currents. In this way the source current are reduced, because the reactive power is compensated and the CS-SAPF contributes with energy from the solar photovoltaic array to the load.

TABLE I
CS-SAPF Simulation Model Parameters

Parameter	Symbol	Value
SAPF dc-link inductance	L_{DC}	200 mH
Passive filter inductor	L_F	0.5 mH
Passive filter capacitor	C_F	10 µF
Passive filter resistance	R_F	0.1 Ω
dc-dc converter inductance	L_{ST}	7 mH
dc-dc converter capacitor	C_{DC}	680 µF
Photovoltaic array short circuit current	i_{SC}	32.4 A
Photovoltaic array open circuit voltage	v_{OC}	526.4 V
Photovoltaic array MPP voltage	v_{MPP}	420.8 V
Photovoltaic array MPP	P_{MAX}	12 kW

TABLE II
Simulation Results when Compensating Full Load

	Source			Load		
Line	Current rms (A)	Current THD (%)	cos φ	Current rms (A)	Current THD (%)	cos φ
a	9.69	4.66	0.99	32.30	11.24	0.82
b	9.63	4.98	0.99	32.30	11.25	0.84
c	9.62	5.08	0.99	32.30	11.23	0.83
Total	-	-	0.99	-	-	0.83

Table II shows the measured results of the simulations. As can be seen, the total harmonic distortion (THD%) of the source currents is lower than the load currents. The power factor is higher in the source. This indicates that the CS-SAPF is operating correctly.

The rms values of the source currents are very low when compared with the load currents. This confirms the statement that the CS-SAPF is injecting energy into the grid and that in the case, this energy is being consumed by the load.

Fig. 7 (a) shows the dc-link current i_{DC}. As can be seen, the dc-link current, although the load is a nonlinear load, has an insignificant ripple. The dc-dc converter capacitor has some influence in this low current ripple. The voltage in this capacitor has also low ripple Fig. 7 (b).

The simulation results of the MPPT algorithm operation are shown in Fig. 8. The figure shows that the MPPT algorithm tracks effectively the operation power of the solar photovoltaic array. In Fig. 7 (b) is possible to see the dc-link capacitor voltage increasing and stabilizing after that is reached to the MPP. The duty-cycle (k_{mpp}) indicates that the MPPT algorithm adjusts the injection of power in the dc-link inductance of the CS-SAPF. Also the voltage in the output of the dc-dc converter, lowers and increases varying according with the duty-cycle. The dc-link current varies according with the loads currents amplitudes that are being compensated. If the amplitude of the currents increases, the dc-link current increases to maintain the modulation index in the linear zone.

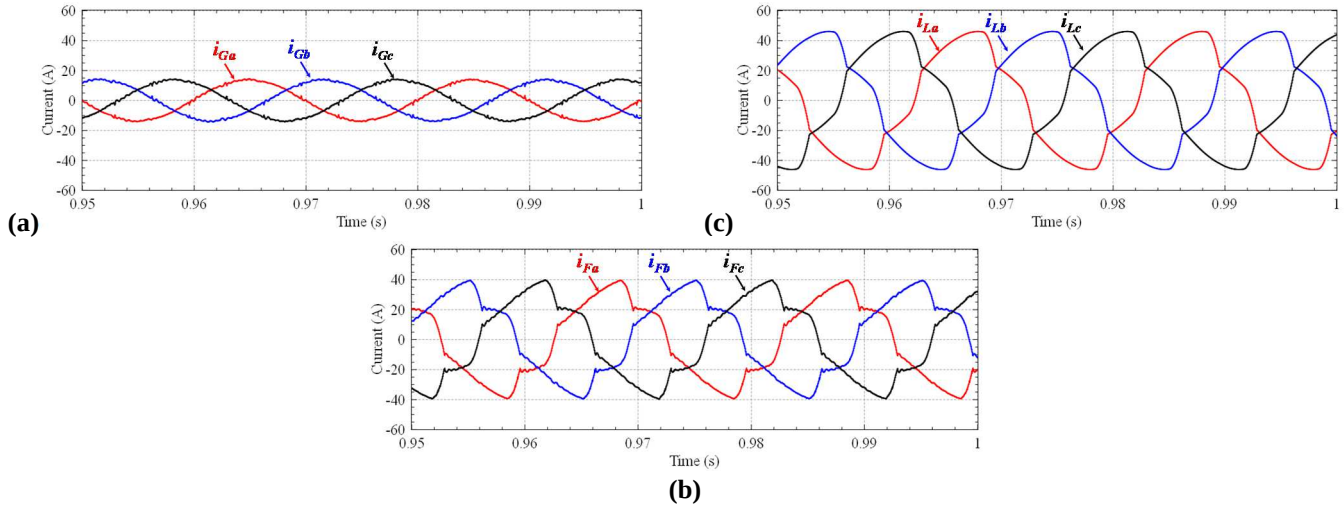

Fig. 6. Simulation results of the CS-SAPF injecting energy from the solar photovoltaic arrays and compensating harmonics and power factor: (a) Grid currents: (b) CS-SAPF currents; (c) Load currents.

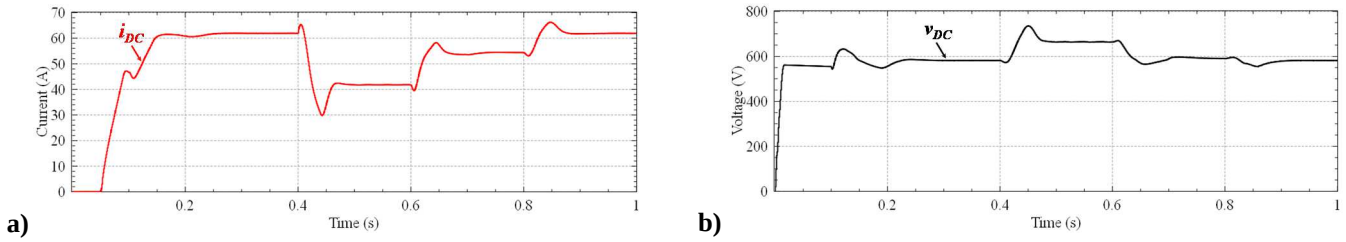

Fig. 7. Dc-link simulation results during load change: (a) Dc-link current; (b) Dc-link voltage.

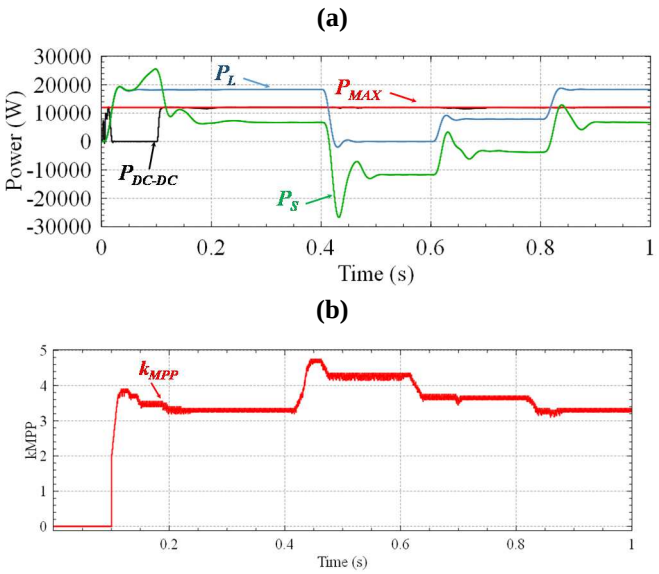

Fig. 8. Simulation results of the MPPT algorithm (a) Dc-dc input power; (b) MPPT control variable.

IV. CONCLUSIONS

In this paper was presented a current-source shunt active power filter (CS-SAPF) that can work simultaneously as active filter (to compensate current harmonics and power factor) and also as interface of solar photovoltaics with the electrical power grid. The paper describes the control algorithms and the power converters that constitute the proposed CS-SAPF. Also are presented the simulation results obtained with the developed model. The simulation results show that the CS-SAPF operates correctly, when compensating nonlinear load harmonics and reactive power, at the same time that injects energy into the electrical power grid. In the future will be implemented a prototype of the proposed equipment in order to obtain experimental results. This will allow to confirm the simulation results and better assess the behavior of the proposed equipment.

ACKNOWLEDGMENT

This work has been supported by FCT – Fundação para a Ciência e Tecnologia within the Project Scope: UID/CEC/00319/2013. Mr. Bruno Exposto was supported by the doctoral scholarship SFRH/BD/87999/2012 granted by FCT.

REFERENCES

[1] J. Holmes, "A More Perfect Union: Energy Systems Integration Studies from Europe," *Power and Energy Magazine, IEEE*, vol. 11, no. 5, pp. 36–45, 2013.

[2] X. Yang, Y. Song, G. Wang, and W. Wang, "A Comprehensive Review on the Development of Sustainable Energy Strategy and Implementation in China," *Sustainable Energy, IEEE Transactions on*, vol. 1, no. 2, pp. 57–65, 2010.

[3] F. Blaabjerg, F. Iov, T. Terekes, R. Teodorescu, and K. Ma, "Power Electronics – Key Technology for Renewable Energy Systems – Status and Future," in *Power Electronics, Drive Systems and Technologies Conference (PEDSTC), 2011 2nd*, 2011, pp. 445–466.

[4] A. E. Jones, M. Irwin, and A. Izadian, "Incentives for microgeneration development in the U.S. and Europe," in *IECON 2010 - 36th Annual Conference on IEEE Industrial Electronics Society*, 2010, pp. 3018–3021.

[5] S. B. Kjaer, J. K. Pedersen, and F. Blaabjerg, "A review of single-phase grid-connected inverters for photovoltaic modules," *Industry Applications, IEEE Transactions on*, vol. 41, no. 5, pp. 1292–1306, 2005.

[6] G. Ertasgin, D. M. Whaley, N. Ertugrul, and W. L. Soong, "A current-source grid-connected converter topology for Photovoltaic systems," in *Australasian Universities Power Engineering Conference. AUPEC'06.(2006: Melbourne, Australia)*, 2006.

[7] B. Sahan, A. Notholt-Vergara, A. Engler, and P. Zacharias, "Development of a single-stage three-phase PV module integrated converter," in *Proc. 12th European Conference on Power Electronics and Applications EPE, Aalborg, Denmark*, 2007.

[8] B. Exposto, J. Pinto, D. Pedrosa, V. Monteiro, H. Goncalves, and J. L. Afonso, "Current-Source Shunt Active Power Filter with Periodic-Sampling Modulation Technique," in *IECON 2012-38th Annual Conference on IEEE Industrial Electronics Society*, 2012, pp. 1274–1279.

[9] Y. Zhang and Y. W. Li, "Investigation and Suppression of Harmonics Interaction in High-Power PWM Current-Source Motor Drives," *Power Electronics, IEEE Transactions on*, vol. 30, no. 2, pp. 668–679, 2015.

[10] G. Ertasgin, "Low-Cost Current-Source 1-ph Photovoltaic Grid-Connected Inverter," 2010.

[11] G.-J. Su and L. Tang, "Current source inverter based traction drive for EV battery charging applications," in *Vehicle Power and Propulsion Conference (VPPC), 2011 IEEE*, 2011, pp. 1–6.

[12] H. Akagi, Y. Kanazawa, and A. Nabae, "Generalized theory of the instantaneous reactive power in three-phase circuits," in *IPEC*, 1983, vol. 83, pp. 1375–1386.

[13] E. H. Watanabe, M. Aredes, J. L. Afonso, J. G. Pinto, L. F. C. Monteiro, and H. Akagi, "Instantaneous p-q Power Theory for Control of Compensators in Micro-Grids," in *Nonsinusoidal Currents and Compensation (ISNCC), 2010 International School on*, 2010, pp. 17–26.

[14] T. Esram and P. L. Chapman, "Comparison of photovoltaic array maximum power point tracking techniques," *IEEE TRANSACTIONS ON ENERGY CONVERSION EC*, vol. 22, no. 2, p. 439, 2007.

[15] M. Salo and H. Tuusa, "A novel open-loop control method for a current-source active power filter," *Industrial Electronics, IEEE Transactions on*, vol. 50, no. 2, pp. 313–321, 2003.